Force and resolution analysis in Kelvin probe force microscopy using nanotube probes

IOP Conf. Series: Materials Science and Engineering **592** (2019) 012036 doi:10.1088/1757-899X/592/1/012036

Force and resolution analysis in Kelvin probe force microscopy using nanotube probes

Jie Xu*, Jianfeng Chen, Long Chen, Yuanlingyun Cai, Tianqi Yu and Jinze Li

College of Electronic and Optical Engineering, College of Microelectronics, Nanjing University of Posts and Telecommunications, Nanjing 210023, China

* E-mail: jiexu@njupt.edu.cn

Abstract. Multiple approaches have been exploited to improve the resolution and sensitivity of Kelvin probe force microscopy (KPFM), among which an apparent method is to use probes with sharp tip apex or with nanotube attached. In this paper, the electrostatic force in KPFM with nanotube probe was calculated by Green's function theorem and boundary element method. Based on the force analysis, the sensitivity and resolution of KPFM using ordinary and nanotube probes were further quantitatively compared with each other. It was found that KPFM measurement with nanotube probe had a better resolution, however, the sensitivity deteriorated under air condition that might constrain its applications.

1. Introduction

Kelvin probe force microscopy (KPFM) has been extensively used to characterize the surface electronic properties of metal, semiconductor and organic samples since its invention in 1990s [1-5]. The KPFM technique has been developed from non-contact atomic force microscopy (AFM), and thus it has a limited resolution due to the long-range electrostatic force between the tip and sample [6-8]. Up till now, several approaches have been proposed to enhance the resolution capability of KPFM. One approach improves the feedback system, e.g., to use frequency modulation (FM) feedback instead of amplitude modulation (AM) so that the signal is sensitive to the more localized force gradient rather than force itself [9], or to use heterodyne AM mode that has a better resolution compared to AM mode and a better sensitivity compared to FM mode [10]. Another approach improves the AFM probe, e.g., to use probes with sharp tip apex or with carbon nanotube (CNT) attached [11].

Here, we focused on the latter approach and precisely calculated the electrostatic force in KPFM with CNT probes by Green's function theorem and boundary element method, through which the sensitivity, point spread function and resolution were quantitatively determined. The result was compared with that of ordinary probes, and the advantage and disadvantage of the measurement with nanotube probes were discussed accordingly.

2. Force analysis in KPFM with CNT probe

The shape of an ordinary silicon probe typically used in KPFM measurement is shown in figure 1(a), and that of CNT attached is shown in figure 1(b). The apex radius and length of silicon tip are 25 nm and 15 m, and those of attached nanotube are 3 nm and 100 nm, respectively. In KPFM measurement, a DC voltage (V_{DC}) is applied between the conductive probe and sample to nullify the local contact potential difference (CPD) by Kelvin feedback controller, and an AC voltage (V_{AC}) is also applied for signal modulation [7]. The electrostatic force under DC bias is essential to the detection signals, so the force analysis is important in the determination of sensitivity and resolution.

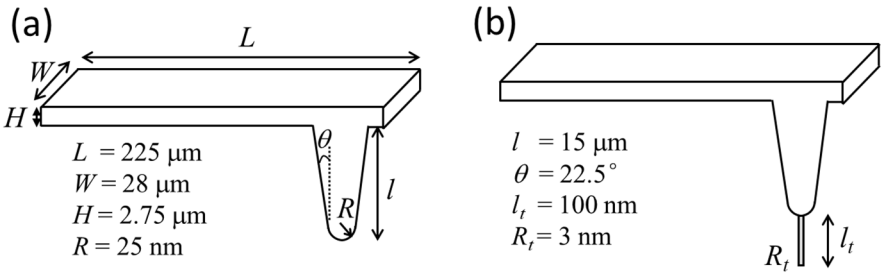

Figure 1. The geometry of (a) an ordinary probe and (b) a CNT attached probe. The size parameters of cantilever (L, W, H) and tip (R, l, , R_t, l_t) are also listed in the inset.

The force in KPFM with ordinary or CNT attached probes can be calculated using Green's function theorem and boundary element method [7, 8]. The main procedure is to calculate a reciprocal Green's function matrix (**G**) and a probe surface-related diagonal matrix (**D**), by dividing the probe surface boundary into N elements first (labeled as S_i, i=1, 2,…N). The **G** matrix is an N by N matrix with its ijth element defined as

$$\mathrm{G}_{ij} = \frac{1}{4\pi\varepsilon_0}\int_{S_j} ds' \left| \boldsymbol{r}' - \boldsymbol{r}_i \right|^{-1} - \left| \boldsymbol{r}' - \tilde{\boldsymbol{r}}_i \right|^{-1}, \tag{1}$$

where $_0$ is the vacuum permittivity, $\boldsymbol{r}_i$ denotes the central position of element S_i, $\tilde{\boldsymbol{r}}_i$ is the image position of $\boldsymbol{r}_i$ with respect to the sample surface, and S_j denotes the jth boundary element related to variables ds' and $\boldsymbol{r}'$. The **D** matrix is an N by N diagonal matrix whose diagonal element is

$$\mathrm{D}_{ii} = \frac{1}{2\varepsilon_0}\int_{S_i} ds' \hat{\boldsymbol{n}} \cdot \hat{\boldsymbol{z}}, \tag{2}$$

where $\hat{\boldsymbol{n}}$ is the normal unit vector of ds', and $\hat{\boldsymbol{z}}$ is the unit vector of z-axis. The electrostatic force on the probe under a DC bias (configuration shown in figure 2(b) inset) is then given by [8]

$$F = (\mathbf{G}^{-1}\vec{\mathbf{I}})^T \mathbf{D}\mathbf{G}^{-1}\vec{\mathbf{I}}V_{DC}^2, \tag{3}$$

where $\vec{\mathbf{I}}$ is an N by 1 vector with identical elements of 1. Notice that the **D** matrix is independent of tip-sample distance, however, the element of **G** matrix increases as the tip-sample distance increases, and therefore the electrostatic force will decrease on the contrary. Moreover, the force gradient can be

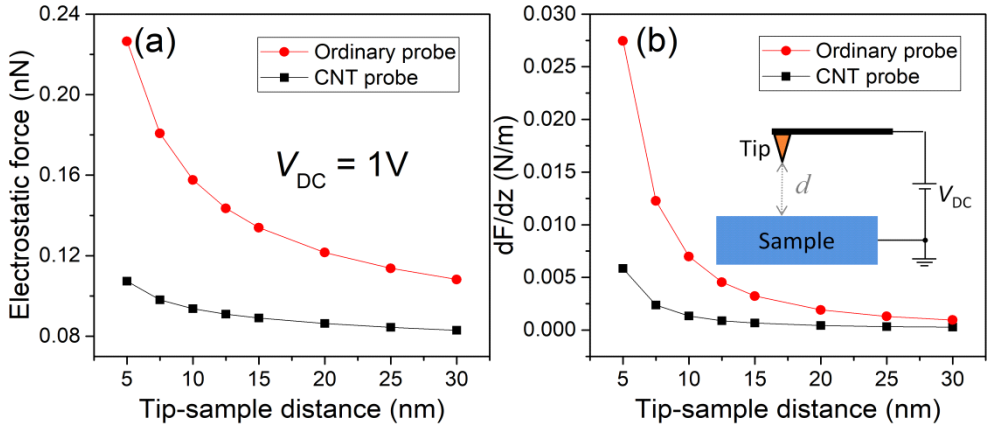

Figure 2. (a) The calculated electrostatic force and (b) force gradient in KPFM with ordinary or CNT attached probes. The tip-sample voltage is kept 1 V in all the calculations.

obtained by the derivative of equation (3), given by

$$\frac{\partial F}{\partial z} = 2\left(\frac{\partial \mathbf{G}^{-1}}{\partial z}\vec{\mathbf{I}}\right)^{T} \mathbf{D}\mathbf{G}^{-1}\vec{\mathbf{I}}V_{DC}^{2}. \tag{4}$$

Figure 2 shows the calculation results of the electrostatic force and force gradient by ordinary and CNT attached probes when the tip-sample bias equals to 1 V. It is shown that the electrostatic interaction is reduced when CNT is attached, due to the smaller effective radius of tip apex. Besides, the variation of force and force gradient of ordinary probe are both larger than those of CNT counterpart when tip-sample distance increases from 5 nm to 30 nm, implying that the detection result using ordinary probe is more sensitive to the tip-sample distance, whereas that using CNT probe is more consistent.

Quantitatively, the sensitivity of KPFM, which is defined as the minimum detectable potential difference, can be obtained by (here we only consider AM mode) [12]

$$\delta V_{CPD} = \frac{kn_z\sqrt{B}}{Q\,|\partial C/\partial z|\,V_{AC}}, \tag{5}$$

where k ans Q are the spring constant and quality factor of the cantilever, n_z is the noise density, B is the bandwidth of the lock-in amplifier, V_{AC} is the AC voltage of KPFM system, and $\partial C/\partial z = 2(\mathbf{G}^{-1}\vec{\mathbf{I}})^{T}\mathbf{D}\mathbf{G}^{-1}\vec{\mathbf{I}}$ is the capacitance gradient that can be deduced from equation (3) (using the relation $F = \frac{1}{2}\partial C/\partial z V_{DC}^{2}$). Figure 3 shows the calculated sensitivity of ordinary and CNT attached probes, where the typical values for the cantilever working in air are used in all the calculations, that is, k = 2.5 N/m, Q = 200, n_z = 100 fm/Hz$^{1/2}$, B = 200 Hz$^{1/2}$, and V_{AC} = 1 V [13]. It is found that CNT probe has a poorer sensitivity than the ordinary counterpart due to the smaller electrostatic interaction as demonstrated in figure 2. A possible way to improve the sensitivity of CNT probes is to use a large V_{AC}, but it may change the electronic states of the sample.

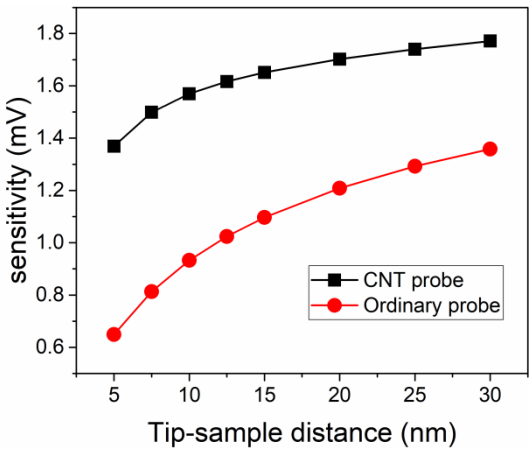

Figure 3. The calculated sensitivity of KPFM measurement using ordinary and CNT attached probes.

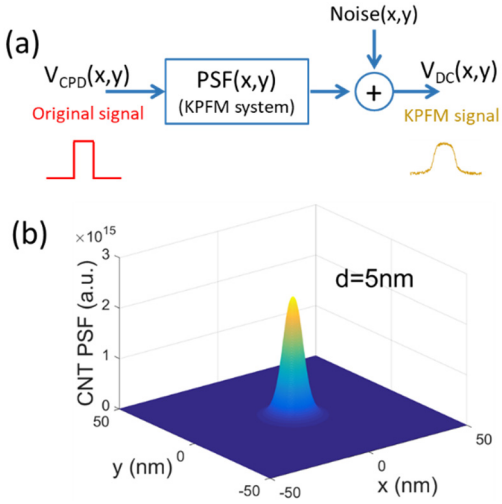

Figure 4. (a) The signal processing diagram of KPFM system; (b) The calculated PSF of CNT probe at tip-sample distance of 5 nm.

3. Resolution analysis in KPFM with CNT probe

Previous electrostatic analysis have shown that the KPFM system is analogous to an optical imaging system that its resolution power can be described by a point spread function (PSF) [7]. The output signal of KPFM is the convolution result of contact potential difference (V_{CPD}) and PSF, as shown in figure 4(a). Considering the system noise, the KPFM signal can be written as

$$V_{DC} = PSF * V_{CPD} + noise. \tag{6}$$

where the asterisk symbol denotes two-dimensional convolution operator. The PSF can be constructed from **G** and **D** matrices [7]

$$PSF(x,y)=[(\mathbf{G}^{-1}\vec{\mathbf{I}})^T\mathbf{D}\mathbf{G}^{-1}\vec{\mathbf{I}}]^{-1}(\mathbf{G}^{-1}\vec{\mathbf{I}})^T\mathbf{D}\mathbf{G}^{-1}\vec{\mathbf{h}}, \quad (7)$$

where **h** is a N by 1 vector whose ith element is $h_i=\frac{z_i}{2\pi}[(x-x_i)^2+(y-y_i)^2+z_i^2)^{-3/2}$, and (x_i, y_i, z_i) is the position of boundary element S_i. An example of PSF matrix with CNT probe is shown in figure 4(b), where the center denotes the tip apex position at x-y plane. Because the **G** matrix is dependent of tip-sample distance, PSF is also tip-sample distance dependent.

Figure 5 shows the profiles of PSFs with CNT probe at different tip-sample distances. If the image is exactly equal to object in the imaging system (i.e., no distortion occurs), the PSF is ideally the Dirac-delta function. Here, the PSF has finite height and width, indicating that the KPFM image (V_{DC}) is distorted from the contact potential difference (V_{CPD}). Besides, the PSF intensity gradually reduces and the full-width at half maximum (FWHM) enlarges as the tip-sample distance increases. The PSF FWHM of ordinary and CNT probes is shown in figure 6, which has been considered as the resolution limit in previous works [7, 8, 14]. The result shows that the resolution limit increases linearly for both probes; therefore, a small tip-sample distance is preferred in KPFM detection in order to obtain good sensitivity and resolution. Besides, the resolution of CNT probe is better than that of ordinary one, in accordance with expected as the attached CNT has much smaller radius of tip apex.

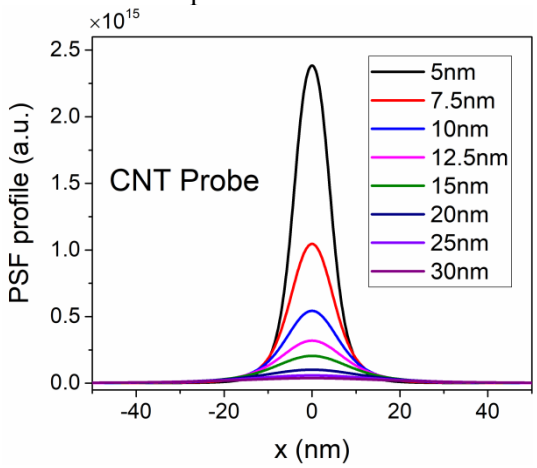

Figure 5. PSF profiles of CNT probe at different tip-sample distances.

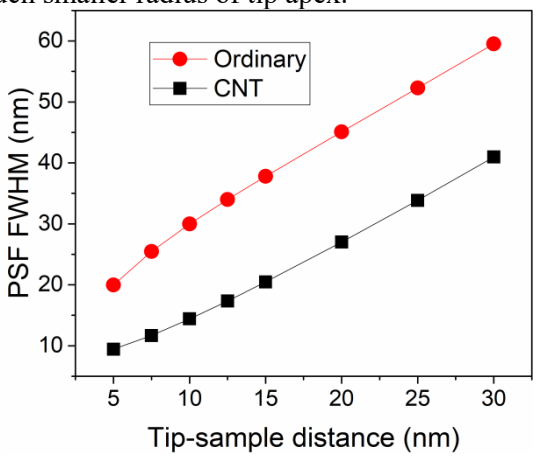

Figure 6. PSF full width at half maximum of ordinary and CNT probes at different tip-sample distances.

4. Conclusion

Nanotube attached probes are thought can enhance the performance of KPFM measurement, and here we analysed the electrostatic force and force gradient in KPFM with ordinary or CNT attached probes, by Green's function theorem and boundary element numerical method. Accordingly, their sensitivity and resolution are quantitatively calculated through linear algebra based algorithm. Calculation results show that the resolution limit can be improved with CNT probe, however, the sensitivity when working in air condition will be deteriorated due to small electrostatic interaction. Moreover, small tip-sample distance is recommended in KPFM measurement with both probes, to obtain better sensitivity and resolution performances.

Acknowledgment

This work was supported by NSFC (No. 61804080), NSF of Jiangsu Province (No. BK20160909) and NUPTSF (No. NY217041).

References

[1] Melitz W, Shen J, Kummel A C and Lee S 2011 Kelvin probe force microscopy and its application *Surf. Sci. Rep.* **66** 1-27
[2] Lan F and Li G 2013 Direct observation of hole transfer from semiconducting polymer to carbon nanotubes *Nano Lett.* **13** 2086-91
[3] Xu J, Li D, Chen D, Li W and Xu J 2018 Nanoscale Characterization of Active Doping Concentration in Boron-Doped Individual Si Nanocrystals *Phys. Status Solidi A* **215** 1800531
[4] Liscio A, De Luca G, Nolde F, Palermo V, Mullen K and Samori P 2008 Photovoltaic charge generation visualized at the nanoscale: a proof of principle *J. Am. Chem. Soc.* **130** 780-1
[5] Xu J, Zheng S, Chen Y, Li W and Xu J 2018 Microscopic and Macroscopic Bipolar Injection and Carrier Recombination in Single-layer Si Nanocrystals *IOP Conference Series: Materials Science and Engineering* **436** 012003
[6] Cohen G, Halpern E, Nanayakkara S U, Luther J M, Held C, Bennewitz R, Boag A and Rosenwaks Y 2013 Reconstruction of surface potential from Kelvin probe force microscopy images *Nanotechnology* **24** 295702
[7] Xu J, Wu Y, Li W and Xu J 2017 Surface potential modeling and reconstruction in Kelvin probe force microscopy *Nanotechnology* **28** 365705
[8] Xu J, Chen D, Li W and Xu J 2018 Surface potential extraction from electrostatic and Kelvin-probe force microscopy images *J. Appl. Phys.* **123** 184301
[9] Ziegler D and Stemmer A 2011 Force gradient sensitive detection in lift-mode Kelvin probe force microscopy *Nanotechnology* **22** 075501
[10] Ma Z M, Mu J L, Tang J, Xue H, Zhang H, Xue C Y, Liu J and Li Y J 2013 Potential sensitivities in frequency modulation and heterodyne amplitude modulation Kelvin probe force microscopes *Nanoscale Res. Lett.* **8** 532
[11] Wilson N R and Macpherson J V 2009 Carbon nanotube tips for atomic force microscopy *Nat. Nanotechnol.* **4** 483-91
[12] Li G, Mao B, Lan F and Liu L 2012 Practical aspects of single-pass scan Kelvin probe force microscopy *Rev. Sci. Instrum.* **83** 113701
[13] Naeli K and Brand O 2009 Dimensional considerations in achieving large quality factors for resonant silicon cantilevers in air *J. Appl. Phys.* **105** 014908
[14] Strassburg E, Boag A and Rosenwaks Y 2005 Reconstruction of electrostatic force microscopy images *Rev. Sci. Instrum.* **76** 083705